Fracture Mechanics of Concrete Structures,
Proceedings FRAMCOS-2, edited by Folker H. Wittmann,
AEDIFICATIO Publishers, D-79104 Freiburg (1995)

MODELLING COMPRESSIVE FAILURE USING RIGID PARTICLE SYSTEMS

Y.-Q. Liu and H. Hikosaka,
Kyushu University, Fukuoka, Japan
J.E. Bolander Jr.,
University of California, Davis, California

Abstract

A rigid particle model is used to simulate mesoscopic failure processes in cement-based composites. Concrete continua are discretized using a large number of Voronoi polygons, each polygon being a rigid element. Concrete is represented using a three component model: cement matrix, aggregate inclusions, and matrix-inclusion interfacial zones. Special attention is given to creating the aggregate inclusions as part of the polygonal mesh. These rigid elements are interconnected by a spring system distributed over the polygon boundaries; spring properties are set according to the component type which they represent. In order to better represent the three-dimensional nature of the material and fracture process, springs properties degrade gradually, based on a measure of damage related to component type. Numerical results are given for different types of loadings, including a uniaxial compression test and a split-cylinder tension test.

1 Introduction

The failure modes of concrete specimens subjected to compression are dependent on the material constituents, specimen geometry and dimensions, and the boundary conditions at the load application points. It is therefore difficult to form consistent interpretations of concrete failure for design purposes. Two main modes of failure are witnessed during testing, those being tensile-type splitting directed along the compression axis and compressive-type diagonal shear failure. However, there are still numerous questions regarding the mechanisms underlying failure, including those concerning the conditions for failure initiation.

Many techniques for analyzing concrete materials, including most finite element approaches, enforce geometric compatibility amongst the model components. Due to these compatibility constraints, such models often have difficulty in simulating failure modes and following the post-peak response. By modeling concrete as an assemblage of rigid bodies interconnected by flexible interfaces (Kawai, 1978), limit state analyses are practicable, while reducing both computational effort and program complexity relative to finite element approaches. The first applications of Kawai's discrete models were to structural analyses, where the usefulness of the approach depends on some a priori knowledge of the failure mode so that the mesh can be aligned accordingly. More recently similar approaches are being applied to modeling microcracking at the material level (Toi and Che, 1993; Toi and Kiyosue, 1995). Here discretizations can be made fine enough so that mesh bias on the fracture directions is minimized.

2 Rigid particle modeling of concrete

A rigid particle model is used to simulate mesoscopic failure processes in cement-based composites. Concrete is represented using a three component model: cement matrix, aggregate inclusions, and matrix-inclusion interfacial zones. The matrix and inclusions are discretized using a large number of Voronoi polygons (Fig. 1), each polygon being a rigid element with two translational and one rotational degrees of freedom.

Aggregate inclusions are randomly positioned within each numerical specimen, satisfying prescribed mix ratios of an actual material. Special attention is given to creating these inclusions as part of the polygonal mesh, as shown in Fig. 1. The points shown in the

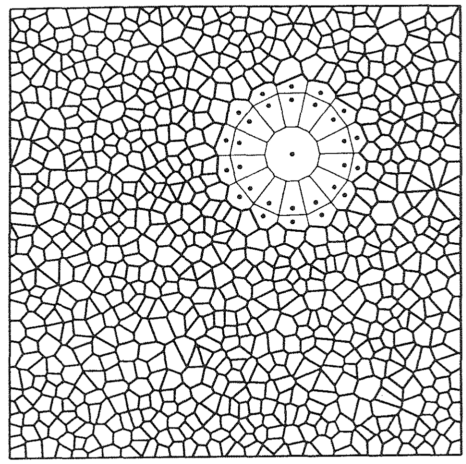

Fig. 1. Circular inclusion in Voronoi polygonal mesh

figure define the aggregate inclusion and are set prior to random generation of the matrix mesh. If the aggregates are strong enough so that they do not fracture before composite failure, then the aggregate can be represented by a single rigid element (instead of the 15 elements shown).

These rigid elements are interconnected by two sets of springs distributed over the polygon boundaries (Kawai, 1978). One set acts normal to the boundaries; the other acts parallel to the boundaries. Spring properties are decided according to the component type which they represent and reflect the properties of the continuum.

In order to better represent the three-dimensional nature of the material and fracture process, springs properties degrade gradually, based on a measure of damage related to component type. For example, tensile fracture of the matrix-inclusion interface is treated as shown in Fig. 2. The first strength limit represents fracture of the interface itself, while the second limit is associated with fracture of yet intact matrix material through the specimen thickness. Over the same interfacial length, fracture along a larger inclusion leads to a greater reduction in local stiffness and strength; interface failure along smaller inclusions has less influence on the local properties. Subsequent fracture events are allowed for modeling additional toughening mechanisms acting through the specimen thickness. While these approaches seem quite simplistic, more rigorous

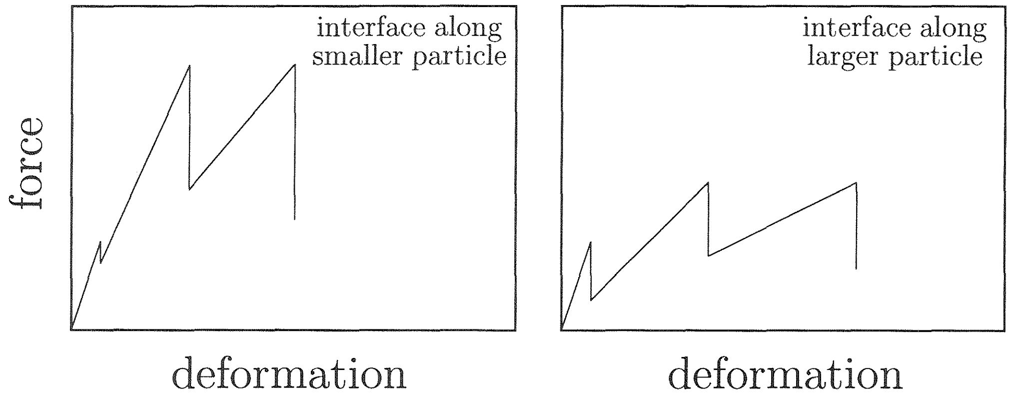

Fig. 2. Tensile fracture along matrix-inclusion interface

modeling strategies may not be warranted given the inadequacies of a two-dimensional analysis framework. It is better to focus our attention on developing fracture models based on three-dimensional discretizations of the material.

3 Compression test simulation

A $10 \times 10 \times 10$ cm concrete specimen is subjected to uniaxial compression, as shown in Fig. 3a. The component tensile strengths are: $f_{\mathrm{ta}} = 6.0$ MPa, $f_{\mathrm{tm}} = 1.5$ MPa, and $f_{\mathrm{ti}} = 1.0$ MPa, where the subscripts a, m, and i denote aggregate, matrix, and interface, respectively. The maximum aggregate diameter is 15 mm. Zero friction is assumed along the loading platform boundaries.

Fig. 4 shows the stress-strain response of the specimen. Cracking initiates along aggregate boundaries at about 30% of the peak load and continues to form with increasing load. At about 80% of peak load, cracks appear in the matrix. The point indicated, just beyond the abrupt drop in load, corresponds to the damage conditions shown in Fig. 3b. As seen in the figure, cracking ultimately tends to be aligned in the direction of compression. Specimen compressive strength, $f_{\mathrm{c}} = 22.5$ MPa, is somewhat strong relative to the assumed component tensile strengths. These results were obtained using a pure tensile fracture criterion; using a Mohr-Coulomb criterion, the peak load can be brought to expected values.

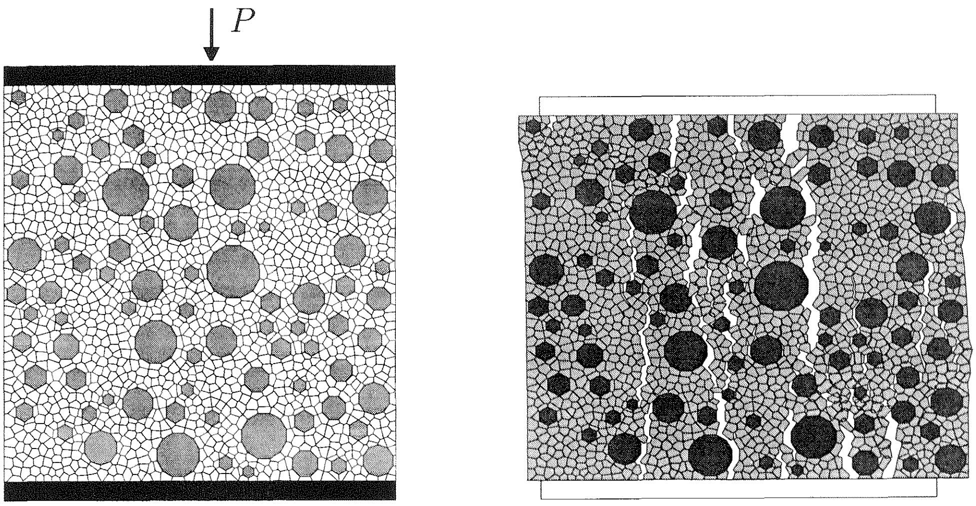

a) undeformed mesh b) post-peak damage condition

Fig. 3. Compression test simulation

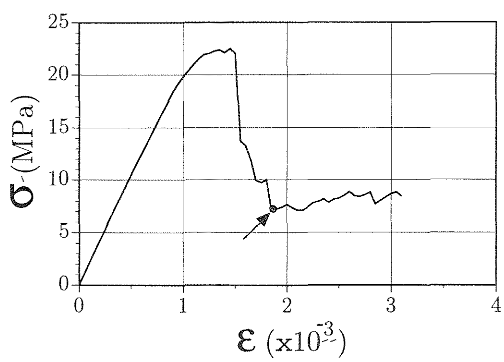

Fig. 4. Compressive stress-strain response

4 Split-cylinder test simulation

As part of a structural test program, a series of split-cylinder tension tests were carried out. The cylinders are 10cm in diameter and 20cm in length. Table 1 shows the maximum load and calculated tensile strength for each test specimen, as well as the average values.

The rigid particle mesh and boundary conditions for the split-cylinder test are shown in Fig. 5a. Aggregate inclusions are distributed in accordance with the mix design. The component tensile strengths are assumed to be: $f_{ta} = 6.0$ MPa, $f_{tm} = 3.0$ MPa, and $f_{ti} = 1.5$ MPa.

Table 1. Split-cylinder test results

specimen	maximum load (kN)	tensile strength (MPa)
1	48.1	1.51
2	57.6	1.83
3	57.9	1.82
average	54.4	1.73

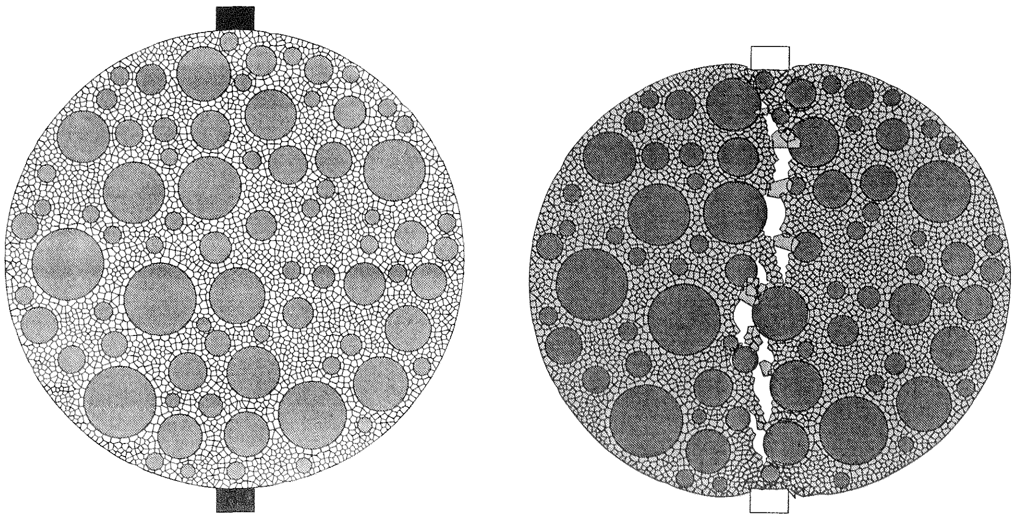

a) undeformed mesh b) post-peak damage condition

Fig. 5. Split-cylinder test simulation

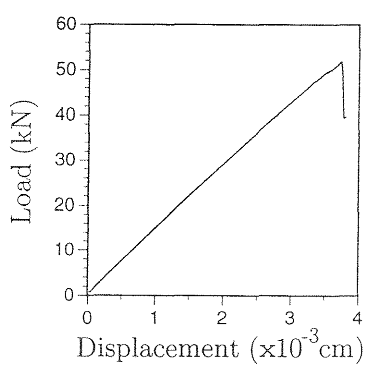

Fig. 6. Load-displacement response

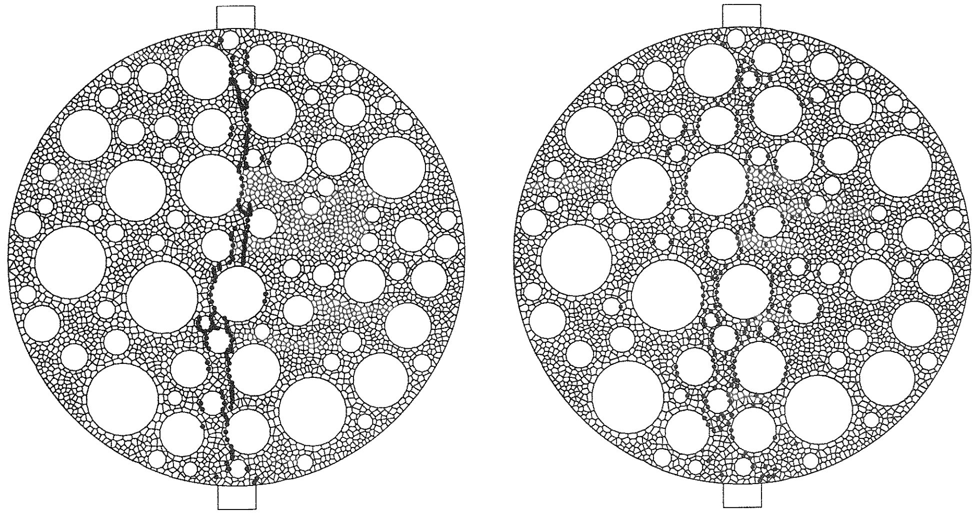

a) complete damage b) partial damage

Fig. 7. Extent of damaged interfaces

Fig. 6 shows the numerical load-displacement response. The peak load of 51.1 kN falls within the experimental scatter. The damage conditions just after peak load are shown in Fig. 5b. (Some elements appear larger than they should due to large rotations.) It seems as if all damage occurs along the main fracture path. The small circles in Fig. 7a show that, indeed, the particle interfaces which have completely failed are close to the main path. However, Fig. 7b shows that the interfaces which have suffered only partial damage cover a broader region.

5 Conclusions

For investigating the fracture properties of concrete, the material mesostructure has been modeled as a system of rigid particles, interconnected by elastic interfaces. This type of modeling is well suited to describing ultimate failure mechanisms and post-peak response, while reducing computational effort and complexity relative to most finite element based approaches. At the same time, however, this model forsakes accurate representation of local strains and stresses. This has implications when trying to model microcrack initiation and propagation under complex loadings, such as in the direct compression test simulation presented in this paper. The model performed better during the split-cylinder test simulation since that type of fracture is driven by a well-defined tensile field.

Though results are realistic in appearance, the usefulness of the approach is greatly limited by the two-dimensional analysis framework. Several assumptions have been made to model three-dimensional features of the material and fracture process, thus detracting from the physical bases we are striving to achieve. Three-dimensional discretizations, which are being carried out by other researchers (albeit at a coarser resolution), are essential to realizing the potential of the rigid particle system approach.

6 References

Kawai, T. (1978) New discrete models and their application to seismic response analysis of structures. **Nuclear Engineering and Design**, 48, 207-229.

Toi, Y., and Che, J.-S. (1993) Mesoscopic simulation of microcracking behaviors of brittle polycrystalline solids. **Proceedings of the Japanese Society of Mechanical Engineers**, 59 (557), 240-247. (in Japanese)

Toi, Y., and Kiyosue, T. (1995) Three-dimensional mesomechanical analysis of brittle solids containing microinclusions. **Proceedings of the Japanese Society of Mechanical Engineers**, 61 (582), 237-243. (in Japanese)